1. Basics

Cartesian tensor and vector notation (see Stull, p. 57-67, for a detailed description)

$\mathbf{x} = x_i = (x_1, x_2, x_3)$

unit vector $\delta_i = (\delta_1, \delta_2, \delta_3)$, in cartesian coordinate normally denoted as (**i**, **j**, **k**)

repeated indices: $x_i\, x_i = (x_1^2 + x_2^2 + x_3^2)$

unit tensor δ_{ij} = 1 for (i=j), and zero for (i≠j)

alternating tensor ε_{ijk} = 1 when the indices are cyclic sequence 1,2,3 or 2,3,1 or 3,1,2;
−1 when indices are not cycline
zero when two indices are the same

vorticity vector $\eta_i \equiv \varepsilon_{ijk}\, \partial u_k/\partial x_j \equiv \partial u_k/\partial x_j - \partial u_j/\partial x_k$

$\mathbf{V} = (\mathbf{u}, w)$, where **u** and w is horizontal and vertical components of winds (currents).

Exercise:

Express or derive the following vector expression by Cartesian tensor

Dot product: $\mathbf{A} \cdot \mathbf{B}$

Cross product: $\mathbf{A} x \mathbf{B}$

Del operator: $\nabla(\,) \equiv$

$\nabla \bullet \mathbf{V}$

$\nabla x \mathbf{V}$

$d/dt = \partial/\partial t + \mathbf{u} \bullet \nabla + w\partial/\partial z$

$\nabla \bullet \nabla x\, \mathbf{V} = \mathbf{0}$

$\nabla x \nabla \varphi = 0$

$\mathbf{V} \bullet \nabla \mathbf{V} = \nabla(\mathbf{V} \bullet \mathbf{V}/2) + (\nabla x \mathbf{V})\, x\, \mathbf{V}$

Governing equations (see Stull, p. 76-78, for a detailed description)

Conservation of matter

$\partial\rho/\partial t + \partial(\rho u_i)/\partial x_i = 0$, where ρ is specific density (mass per unit of volume)

Momentum

$\partial u_i/\partial t + u_j \partial u_i/\partial x_j + 2\varepsilon_{ijk}\Omega_j u_k = -\rho^{-1}\partial p/\partial x_i - \partial\Phi/\partial x_i + \rho^{-1}\partial\tau_{ij}/\partial x_j$

$\Omega_j = (0, \omega\cos\varphi, \omega\sin\varphi)$, components of the angular velocity of the earth's rotation vector, where φ is latitude and $\omega = 2\pi$ / 24 hr = $7.27 \times 10^{-5}\ s^{-1}$

Coriolis parameter $f = 2\omega\sin\varphi$, $f_c = 2\omega\cos\varphi$

$\tau_{ij} = \mu\,(\partial u_i/\partial x_j + \partial u_j/\partial x_i) + (\mu - \mu_B)\, \partial u_k/\partial x_k\ \delta_{ij}$

μ: dynamic viscosity, $\nu = \mu/\rho$ kinematic viscosity, μ_B ~bulk viscosity coefficient

μ_B ~0 for most gases & assuming incompressibility $\rho^{-1}\partial\tau_{ij}/\partial x_j \approx \nu\partial^2 u_i/\partial x_j^2$

In vector form, $\mathbf{V} = (\mathbf{u}, w)$, the momentum equation can be written as

$d\mathbf{u}/dt + f\, \mathbf{k} x\, \mathbf{u} = -\rho^{-1}\nabla p + \nu(\nabla^2 + \partial^2/\partial z^2)\mathbf{u}$

$dw/dt + f_c\, \mathbf{i} \bullet \mathbf{u} = -\rho^{-1}\partial p/\partial z - g + \nu(\nabla^2 + \partial^2/\partial z^2)w$

Home work: find the values of ν and μ for air and water

<u>Energy</u>

Mechanical energy

$u_j \partial u_i / \partial x_j = \partial(u_j u_j/2)/\partial x_i + \varepsilon_{ijk} \eta_j u_k$ [$\mathbf{V} \bullet \nabla \mathbf{V} = \nabla(\mathbf{V} \bullet \mathbf{V} /2) + (\nabla \times \mathbf{V}) \times \mathbf{V}$]

ρu_i [$\partial u_i/\partial t + \partial (u_j u_j/2 + \rho^{-1} p + \Phi) / \partial x_i + \varepsilon_{ijk}(\eta_j + 2\Omega_j) u_k - \rho^{-1} \partial \tau_{ij}/\partial x_j = 0$]

$\rightarrow \partial(\rho e)/\partial t = -\partial [u_i(\rho e+p) - u_j \tau_{ij}] / \partial x_i - \rho u_i \partial \Phi/\partial x_i + p \partial u_i/\partial x_i - \tau_{ij} \partial u_j/\partial x_i$

where $e = u_j u_j/2 = \mathbf{V} \bullet \mathbf{V} / 2$, incompressibility

$\tau_{ij} \partial u_j/\partial x_i = \tau_{ij} \partial u_i/\partial x_j = \tau_{ij}(\partial u_i/\partial x_j + \partial u_j/\partial x_i)/2 = \rho \nu (\partial u_i/\partial x_j + \partial u_j/\partial x_i)^2/2 \equiv \rho \varepsilon$

Deriving the above equation in vector notation, $\rho \mathbf{u} \bullet [\partial \mathbf{u}/\partial t + ...] + \rho w [\partial w/\partial t + ..]$,
And the following identities:

$\nabla \bullet \nabla \times \mathbf{V} = \mathbf{0}$; $\nabla \times \nabla \varphi = 0$; $\mathbf{V} \bullet \nabla \mathbf{V} = \nabla(\mathbf{V} \bullet \mathbf{V} /2) + (\nabla \times \mathbf{V}) \times \mathbf{V}$

$\partial(\rho e)/\partial t$: storage term

$[u_i(\rho e+p)]$: Energy flux produced by the total pressure (dynamic and static)

$[-u_j \tau_{ij}]$: Viscous energy flux produced by molecular scale stresses (small)

$\rho u_i \partial \Phi/\partial x_i = \rho w g$: work of gravity due to vertical motion

$p \partial u_i/\partial x_i$: work of pressure due to expansion or compression

$\tau_{ij} \partial u_j/\partial x_i \equiv \rho \varepsilon$: ε is dissipation rate per unit mass

Turbelence and turbulent transport

<u>Separation of variables:</u>

fluid motions and associated thermodynamic states are separated into a slowly varying mean flow and a rapidly varying turbulent component. The averages of variables will be taken in time, assuming that this will be a good representation of ensemble average. Thus $u = \bar{u} + u'$, and the mean of $u' = 0$.

The <u>mean of mass conservation</u>, $\partial \rho/\partial t + \partial(\rho u_i)/\partial x_i = 0$

$\rightarrow \quad \partial \bar{r}/\partial t + \partial(\bar{r} \bar{u}_i)/\partial x_i = 0$

The <u>mean of momentum equation</u>

$$\partial u_i/\partial t + u_j \partial u_i/\partial x_j + 2e_{ijk} \Omega_j u_k = -r^{-1} \partial p/\partial x_i - \partial \Phi/\partial x_i + r^{-1} \partial t_{ij}/\partial x_j$$

$$\rightarrow r\left(\partial \bar{u}_i/\partial t + \bar{u}_j \partial \bar{u}_i/\partial x_j + 2e_{ijk} \Omega_j \bar{u}_k\right) = -\partial \bar{p}/\partial x_i - r\, \partial \Phi/\partial x_i - \partial\left[r\left(\overline{u_j' u_i'} - v \partial \bar{u}_i/\partial x_j\right)\right]/\partial x_j$$

where $-r\left(\overline{u_j' u_i'} - v \partial \bar{u}_i/\partial x_j\right) \equiv t$,

The horizontal component of the above equation can be expressed as

$$\left(d\bar{u}/dt + f \quad k \times \bar{u}\right) = -r^{-1} \nabla \bar{p} + r^{-1} \partial t/\partial z \,,$$

where $t = -r\left(\overline{u' w'} - v \partial \bar{u}/\partial z\right)$ with the horizontal stress variations neglected.

The mean of K.E. equation

(1) $\overline{\partial(re)/\partial t = -\partial[u_i(re+p)-u_j t_{ij}]/\partial x_i - r u_i\,\partial\Phi/\partial x_i - re}$

$\rightarrow$ an equation for the averaged local change of K.E. per unit mass

(2) scalar multiplication of the above mean momentum equation with the mean velocity $\bar{u}_i$

$\rightarrow$ an equation for the work done by the averaged velocity

If this second equation is subtracted from the first, we get a TKE equation

<u>Turbulence Kinetic Equation (TKE)</u>

$$\partial e/\partial t = -\overline{u_i'u_j'}\,\partial\bar{u}_j/\partial x_i - g\,\overline{r'w'}/r - \partial\left[\bar{u}_i\bar{e} + \overline{u_i'(e+p'/r)}\right]/\partial x_i - e$$

where $\bar{e} = \left(\overline{u_i'u_j'}\right)/2$, molecular stress τ_{ij} is assumed small compared to the Reynolds stress, and that the dissipation acts only on the eddying motion and that its direct effect on the mean velocities negligible:

$$e \approx \overline{v\left(\partial u_i'/\partial x_j + \partial u_j'/\partial x_i\right)\partial u_j'/\partial x_i} \qquad 0 \approx v\left(\partial\bar{u}_i/\partial x_j + \partial\bar{u}_j/\partial x_i\right)\partial\bar{u}_j/\partial x_i$$

The TKE can be simplified by neglecting all eddy transport except those along the vertical

$$\partial\bar{e}/\partial t = -\overline{w'u'}\bullet\partial\bar{u}/\partial z - g\,\overline{r'w'}/r - \partial\left(\overline{w'e} + \overline{w'p'}/r\right)/\partial z - e$$

$\overline{w'u'}\bullet\partial\bar{u}/\partial z$: shear production term of TKE by the reduction of the mean shear

$-g\,\overline{r'w'}/r$: work of buoyancy force

$\partial\left(\overline{w'e}\right)/\partial z$: a transport of TKE by turbulent eddies

$\partial\left(\overline{w'p'}/r\right)/\partial z$: energy flux associated with pressure fluctuations

ε: dissipation

For a derivation of TKE equation, see Stull p.116, p.120-124

See Stull p.153-166

Equations similar to the TKE equation may be constructed for all second-order turbulent variables such as $u_i'u_j'$ ($u_i'u_i'$ is a special case of this), θ′θ′, w′θ′, w′q′, etc.

$\overline{w'u'} = -k_m\,\partial\bar{u}/\partial z$, $\overline{w'q'} = -k_T\,\partial\bar{q}/\partial z$, $\overline{w'q'} = -k_e\,\partial\bar{q}/\partial z$

where k_m, k_T, k_e are eddy transfer coefficients that have the same dimension as the molecular diffusivity or viscosity, but their value is generally much larger and they are not intrinsic properties of the fluid. Unlike the molecular coefficients, they vary with the location, the state of the fluid, the stability and the averaging period. When the mean gradient becomes zero, the representation of transports by the above expression makes no sense.

TKE budget as a function of eddy size

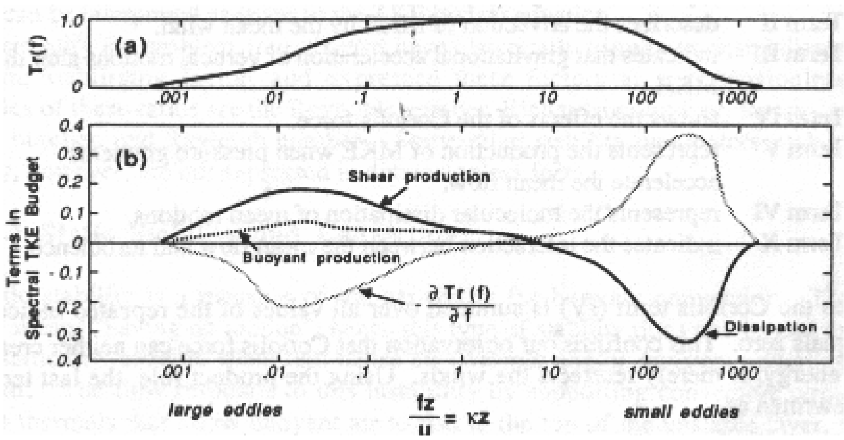

Inertial subrange

Fig. 1 Example of spectral energy budget terms for z/L =-0.29. Shown in (b) are the shear and buoyancy production and the dissipation terms as functions of frequency f. The shaded curve (labeled ¶Tr(f)/¶f) is equal to minus the sum of the shar, buoyancy production and dissipation terms. The Tr(f) curve (a) was obtained by integrating ¶Tr(f)/¶f. Here Tr(f) is the transfer of energy in f space required to balance the production and dissipation. The symbol f is frequency and k is wave number. After McBean and Elliott (1975). Such transfer can be thought of as happening inertially-large eddies creating or bumping into smaller ones, and transferring some of their inertia in the process. This middle portion of the spectrum is called ***inertial subrange****.*

One measure of the smallest scales of turbulence is the Komogorov microscale by: $\eta = (\nu^3/\varepsilon)^{1/4}$. This scaling assumes that the smallest eddies see only turbulent energy cascading down the spectrum at rate ε, and feel only the viscous damping ν.
$\nu = 10^{-5}$ $m^2 s^{-1}$ for air viscosity
$\varepsilon = u^2$ u/L, where u and L are the velocity and length scale of the energy-containing eddies. For a convective ABL, u ~ w_* ~1 ms^{-1}, and L ~ z_i ~ 1 km (ABL depth), hence
$\varepsilon = 10^{-3}$ $m^2 s^{-3}$
$\eta = (\nu^3/\varepsilon)^{1/4} = 10^{-3}$ m, so turbulent eddies in the ABL range from km to mm in scale. The largest eddies are responsible for most of the turbulent transport of heat, moisture, and momentum, small eddies are mainly dissipative.

The spectral distribution of energy for this subrange can be obtained following dimensional consideration. Let dE=F(k)dk, where k is the wavenumber and dE is the energy for the spectrum range between k and k+dk. Then F(k) has the dimension of $L^2T^{-2} / L^{-1}=L^3T^{-2}$. If we assume F(k)= $\varepsilon^m k^n$, $L^3T^{-2}=L^{2m}T^{-3m}L^{-n}$. From this we obtain m=2/3 and n=-5/3 and thus **F(k)=** $a\,e^{2/3}\mathbf{k}^{-5/3}$, where α is a universal constant.

TKE spectra and some observational means to measure it

1. Optical measurements of breaking wave turbulence
   <http://www.udel.edu/ASI-Lab/research/dopplerbreakwave.html>

With the development of DPIV techniques that provide improved spatio-temporal coverage measurements, we considered it timely to once again return to a study of the unsteady breaking of individual waves. In this study we use DPIV techniques to measure the velocity and vorticity fields under breaking waves in the laboratory. We use the dispersive focussing technique to generate intermediate or long packets of deep-water waves. Thus the conditions of the experiments could correspond to the breaking of wind waves and swell on the continental shelf, where the depth is not directly important for the individual waves but may be for the long waves forced by the modulation of the carrier waves. Despite the spatial coverage provided by imaging techniques like DPIV, we found that we could not cover the full dynamic range and spatial extent of the flow in one image frame. While the desire to directly measure the smallest turbulent (Kolmogorov) scales would have required frame sizes of O(1) cm, the desire to image the whole flow would have required frames of O(1) m. We concluded that detailed studies at the Kolmogorov scales were premature before the overall kinematics of the flow were measured, and so we decided to conduct a series of measurements designed to characterize the larger coherent structures in the flow and look at the integral properties of the flow based on the energy bearing scales. Even with this decision it was not possible to image the whole flow with sufficient spatial resolution and we decided to build up a "picture" of the whole flow with a "mosaic" of individual frames. Since each realization of the flow is unique, such a scheme depends on our ability to build up the coherent features of the flow and the statistics through ensemble averaging.

Figure 1 shows ensemble average of the mean velocity vectors, the streamlines (along with the magnitude of the velocity) and the turbulent kinetic energy were the turbulent velocity is calculated as the departure from the ensemble mean. We have shown that an overall description of the turbulence and coherent structures generated by breaking waves in the laboratory can be studied using a mosaic of smaller DPIV images. The advances in imaging systems since these experiments were conducted would permit a finer resolution of the velocity field with fewer fields of view, but it is likely that this mosaic approach will still be required to fully represent the flows associated with breaking waves of large Reynolds numbers.

We find that the coherent vortex generated by the breaking wave advects slowly in the wave propagation direction with a speed of approximately 0.01C, for at least 50 periods after breaking. This is consistent with the speed induced by an image line vortex above the free surface. The speed of the vortex corresponds to the speed at which the fields of turbulent kinetic energy and vorticity propagate downstream. We show that this vortex, through well-established mechanisms of wave-current interaction, may lead to a persistent region of smooth water at the site of breaking in the field.

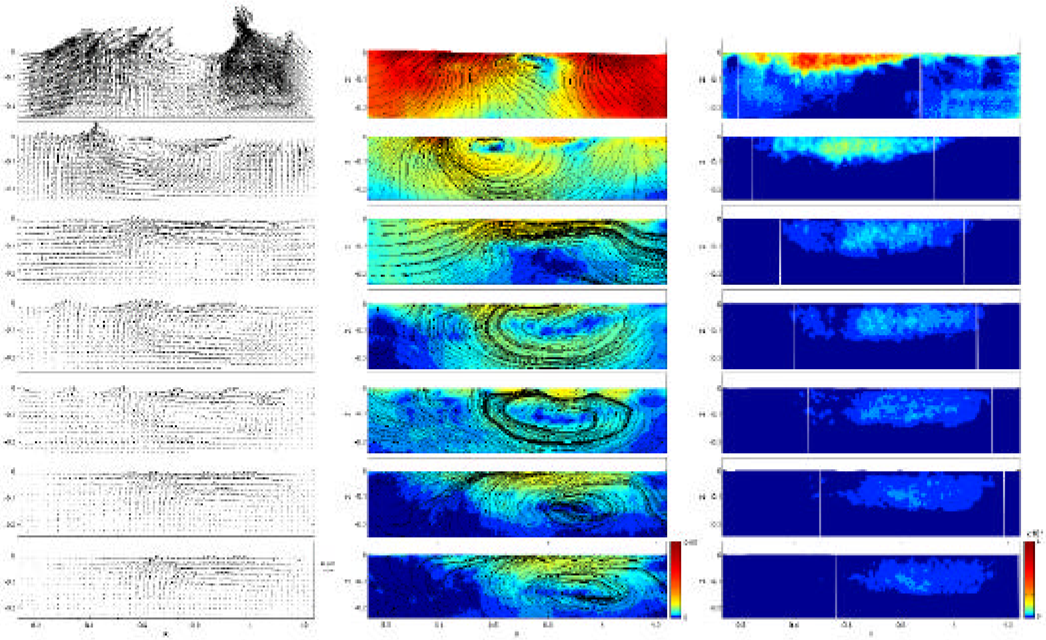

Figure 1 a) Mean velocity under a breaking wave at different times after the breaking event. Note the mean vortex propagating downstream. b) Streamline of the mean flow presented in a). c) turbulent kinetic energy density of the turbulence. The high levels of turbulence initially generated quickly dissipate.

Our measurements of the kinetic energy and vorticity, and the Reynolds stress, show that they decay like t-1, consistent with the earlier measurements of Rapp and Melville (1990) and the recent numerical modeling by Chen et al. (1999).

Measurements of the Reynolds stress, along with the hypothesis of Reynolds number independence for large R, can be used to estimate the momentum flux from breaking waves into the water column. These estimates are consistent with our earlier measurements described in Melville (1994), but are an order of magnitude less than those implied by the quasi-steady breaking measurements of Duncan (1981,1983), and an order of magnitude larger than those estimated by Phillips et al. (1999) on the basis of field measurements of microwave scattering by breaking waves. These discrepancies need to be resolved.

2. Acoustic Doppler measurements of breaking wave turbulence
<http://www.udel.edu/ASI-Lab/research/dopplerbreakwave.html>

An improved understanding of turbulence and mixing due to wave breaking is essential for progress in a number of areas of air-sea interaction. For surface waves, breaking is normally considered to be a sink of energy (and action); although, like any disturbance, it may also be a source. Breaking, as a dissipative mechanism when momentum is conserved, leads to the generation of currents. The details of the near-surface currents depend on the fact that breaking is a source of turbulence for the upper mixed layer, and may lead to departures from classical law-of-the-wall velocity profiles. Fluxes of heat and gas across the air-sea interface, which are so important for weather and climate up to global scales, depend on the levels of surface turbulence, which are due in part to breaking. Bubbles entrained by breaking may also contribute to gas transfer, and their contribution depends on the depths to which they are mixed by the surface currents and turbulence. Breaking provides strong signatures in remote sensing of the ocean surface; signatures that depend on processes of wave-current interaction associated with wave breaking. For these reasons and more, an improved knowledge of the fluid dynamics of breaking is vital to a better understanding of air-sea interactions from micro- to global scales (Banner and Peregrine, 1993; Melville, 1996).

The surface-wave zone or upper surface mixed layer of the ocean has received considerable attention in recent years. This is partly a result of the realization that wave breaking (Thorpe 1993, Melville 1994, Anis and Moum 1995) and perhaps Langmuir circulations (Skyllingstad and Denbo 1995, McWilliams et al. 1997, Melville et al. 1998) may lead to enhanced dissipation and significant departures from the classical ``law-of-the-wall'' description of the surface layer (Agrawal et al. 1992, Craig and Banner 1994, Terray et al. 1996). The classical description would lead to the dissipation, ε, being proportional to z^{-1}, where z is the depth from the surface, whereas recent observations show $\varepsilon \sim z^{-2}$ to z^{-4} (Gargett 1989, Drennan et al. 1992), or $\varepsilon \sim e^{-z}$ (Anis and Moum 1995), with values of the dimensionless dissipation (where κ is Von Karman constant and u*w the friction velocity in water) up to two orders of magnitude higher than the O(1) expected for the law of the wall (Melville 1996). Since dissipation estimates are made from measurements over the inertial or dissipation subranges of the turbulent scales, it would be desirable to avoid any form of Taylor's hypothesis and have an instrument that could make direct spatial (wavenumber) measurements over these ranges in the field. To our knowledge, the only means of making dense spatial measurements of velocities are either optical or acoustical. Experience in the laboratory with Laser Doppler Velocimetry (LDV) (Rapp and Melville 1990) and Digital Particle Imaging Velocimetry (DPIV) (Melville et al. 1998) led us to believe that optical techniques, while very attractive, may be less robust than acoustical systems in the active wave zone of the ocean. Accordingly, we decided to pursue acoustical techniques.

The experiments were performed in the 28.7 m-long glass-walled wave channel at the Scripps Institution of Oceanography. The tank is 0.5 m wide and was filled with fresh water to a depth of 0.6 m. Waves were generated by a hydraulic paddle that sent a packet consisting of high frequency waves followed by low frequency waves so that constructive interference leads to breaking at a time tb at a predetermined location xb along the channel (see Rapp and Melville 1990, Loewen and Melville 1991 for details). The velocity under breaking waves was measured using a pulse coherent Doppler sonar with a range resolution of 1 cm. Figure 2 shows the velocity under a typical breaking event measured with the Doppler and a PIV system. It appears that most of the velocity field can be identified as either orbital motion due to surface waves or turbulence.

Using two dimensional Fourier techniques, it is possible to decouple the turbulence from the wave motion. It is then possible to use common statistical tools to analyze the turbulence created by the breaker (Tennekes and Lumley 1972). Figure 2c shows the wavenumber spectrum calculated on the velocity of figure 2a and b and shows a well define inertial subrange in the turbulence. We have then used the inertial subrange of the spectrum to determine ε directly.

This acoustical technique was also extended to the field where we have measured the velocity wavenumber spectra in the upper 40 cm of the ocean under various wind and wave conditions. It was found that the kinetic energy dissipation levels were consistent with a layer of enhanced turbulence levels near the surface (Fig. 3).

The Doppler was subsequently deployed in the surf zone were it demonstrated its ability to resolve fluid velocity in extreme conditions and showed that it could be potentially employed in a wide range of applications.

We have presented tests of a pulse-to-pulse coherent acoustic Doppler profiler in both the laboratory and the field. It has been stated that the main advantage of the Dopbeam over conventional single point velocity measurements is the ability to acquire profiles of the fluid velocity with a high sampling rate which leads to two-dimensional data where the fluid velocity is a function of range and time. We have seen that this permits the study of turbulence in great detail and the collection of flow statistics as a function of time. In the laboratory, direct comparisons of velocity and wavenumber spectra from the Dopbeam and DPIV measurements are very good. A two-dimensional Fourier transform of the data shows a fairly clear separation of the turbulence and the wave field, allowing for appropriate filtering. Spectrograms of the turbulence generated by breaking waves show the accelerating propagation of the spectral peak with time toward higher wavenumbers (i.e. the breakdown of energy containing eddies into smaller scales). Averaging the wavenumber spectrogram of a breaking event over time yields a single wavenumber spectrum. Breaking waves of varying strength were studied and the spectra obtained exhibit a -5/3 spectral slope, the signature of the inertial subrange in the turbulence. Identifying the inertial subrange, and measuring the spectral level permits direct estimates of the turbulent kinetic energy dissipation e under breaking waves. In the field, analysis of the data shows that the instrument can measure wavenumber spectra and resolve the inertial subrange over wavelengths in the range O(0.01-1) m, demonstrating its use for measuring turbulent dissipation in the upper mixed layer/surface-wave zone. Since, any form of Taylor's hypothesis is avoided by the direct spatial measurement, the instrument is not limited to wave conditions which satisfy the requirements of a frequency-wavenumber transformation. One limitation of the instrument, however, is that it requires the presence of an inertial subrange in the turbulence in order to be able to measure the dissipation rate. We conclude that the instrument may prove useful for direct field measurements of turbulent wavenumber spectra.

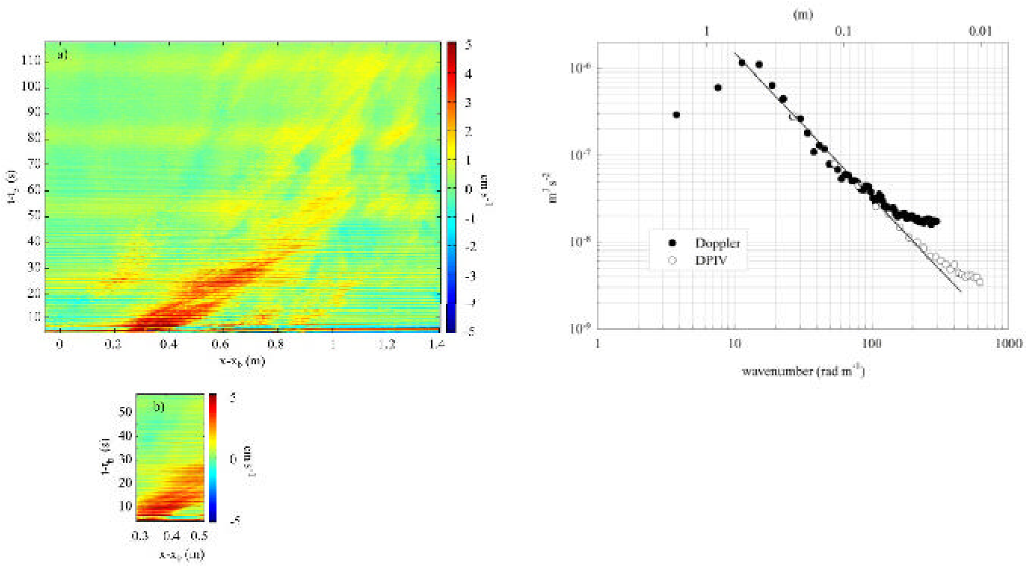

Figure 2 Example of velocity data recorded by the Dopbeam a) and the DPIV b) for a breaker with a slope of S=0.656. The color code is the downstream velocity in cm/s. The horizontal axis represents the downstream distance from the location of the breaker xb, and the vertical axis is the time elapsed from tb, the time of the breaking event. c) Corresponding wavenumber spectra. The solid line has a -5/3 slope.

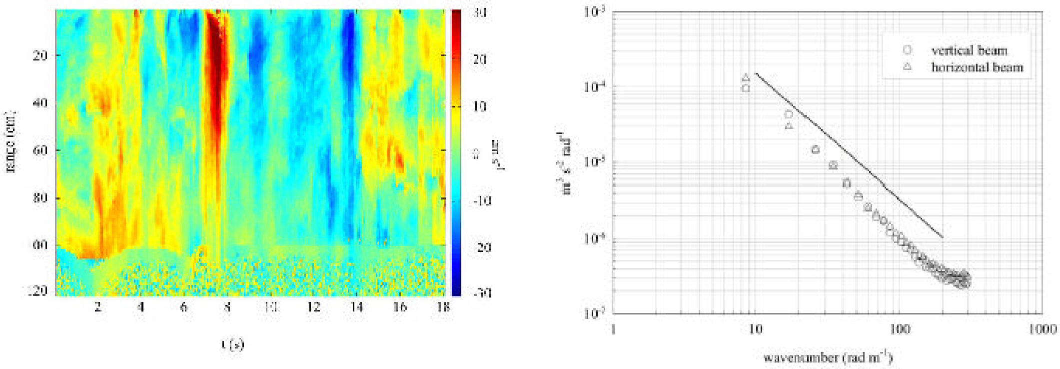

Figure 3 a) Example of the vertical velocity recorded by the Dopbeam in the surf zone. Note that the bottom is apparent at a range of approximately 1 m. b) Wavenumber spectra for both orientation of the Dopbeam in the surf zone. The solid line has a -5/3 slope.

3. On probing the inertial subrange.

Henjes, K., 1999: On probing the inertial subrange. *Boundary-Layer Meteorology* **91**(3), 367 - 384.

Abstract

For an extensive turbulent wind speed data set collected on the open ocean, the optimum sampling time is determined to calculate inertial-range spectra. This time interval, ca. 6s, corresponds to the turbulent memory time, the minimum period after which a given time series can be interpreted as a new independent measurement.

Separate spectral levels are calculated from the 3 measured vector components. Their ratios are compatible with the assumption of an isotropic inertial subrange, but scatter considerably. Alignment factors are developed based on Kolmogorov's theory, and the aligned spectral levels coincide within a few percent. It is proposed that alignment might be a better test for inertiality than the ratio of the spectral levels.

4. Simulation of the Kolmogorov inertial subrange using an improved subgrid model

Chasnov, J. R., 1991: Simulation of the Kolmogorov inertial subrange using an improved subgrid model. *Phys. Fluids.* **A3**(1)

Statistical description of fluctuating quantities

<u>Correlation function and spectra</u>

<u>Isotropic turbulence</u>

Scaling technique

$x, y, z = (Lx^*, Ly^*, Dz^*)$, $t = \omega^{-1}t^*$
$u, v, w = (Uu^*, Uv^*, UDL^{-1}w^*)$

Vertical momentum equation

$dw/dt + f_c\, \mathbf{i} \bullet \mathbf{u} = -\rho^{-1}\partial p/\partial z - g + \nu(\nabla^2 + \partial^2/\partial z^2)w$ $[\partial p/\partial z + \rho g = \partial p'/\partial z + \rho' g,\ b' = -g\rho'/\rho_0]$
$dw/dt + f_c\, \mathbf{i} \bullet \mathbf{u} = -\rho_0^{-1}\partial p'/\partial z + b' + \nu(\nabla^2 + \partial^2/\partial z^2)w$
$[\ \partial/\partial t^* + u^* \bullet \nabla^* + w^*\partial/\partial z^* - (D^2/L^2\nabla^{*2} + \partial^2/\partial z^{*2})\ ]\ w^* = \ (1+1/\rho_s\, b'\, \partial p'/\partial z)$
$D/L\ [\ \omega U/b' \qquad U^2/Lb' \qquad \nu U/D^2 b' \qquad]$

Reynolds number: $Re = UL/\nu$ $[\ U/L : \nu/D^2 = UL/\nu\ (D/L)^2\ ]$

$U \propto D^2 b'/\nu$

Froude number: $Fr = -U^2/Lb'$

Horizontal momentum equation

$d\mathbf{u}/dt + f\, \mathbf{k} \times \mathbf{u} = -\rho^{-1}\nabla p + \nu(\nabla^2 + \partial^2/\partial z^2)\mathbf{u}$
$[\ \partial/\partial t^* + \mathbf{u}^* \bullet \nabla^* + w^*\partial/\partial z^* - (D^2/L^2\nabla^{*2} + \partial^2/\partial z^{*2})\ ]\ \mathbf{u}^* = \ f\, \mathbf{k} \times (\mathbf{u}^* - \mathbf{u}_g^*)$
$[\ \omega/f \qquad U/fL \qquad \nu/D^2 f \qquad]$

Rossby number: $Ro = U/fL$

Ekman number: $Ek = \nu/D^2 f = Ro/Re\ (D/L)^2$

TKE equation

$$de/\partial t = -\overline{w'u'} \bullet \partial\bar{u}/\partial z - g\,\overline{r'w'}/r - \partial\left(\overline{w'e} + \overline{w'p'}/r\right)/\partial z - e$$

Flux Richardson number: $Rf = \left(-g\,\overline{r'w'}/r\right)/\left(\overline{w'u'} \bullet \partial\bar{u}/\partial z\right)$
Normally $w'\mathbf{u}' \bullet \partial\mathbf{u}/\partial z < 0$ and $-g\rho' w'/\rho = b'w'$ can be positive or negative,
When $b'w'$ is positive, flow is turbulent
When $b'w'$ is negative, then

$Rf < 1$ flow is turbulent (dynamically unstable)

$Rf > 1$ flow becomes laminar (dynamically stable)

Gradient Richard number: $Ri = (-g\,\rho^{-1}\,\partial\rho/\partial z) / (\partial \mathbf{u}/\partial z) \bullet (\partial \mathbf{u}/\partial z)$

$Ri < Rc$ laminar flow becomes turbulent ($Rc = 0.21 \sim 0.25$)

$Ri > R_T$ turbulent flow becomes laminar ($R_T = 1.0$)

Hysteresis effect:

Ri of nonturbulent flow must be lowered to Rc before turbulence will start, but once turbulent, the turbulence can continue until the Ri is raised above R_T

(Kekvin Helmholtz instability, see Stull p. 172-173)

Bulk Richardson number: $Rb = (-g\,\rho^{-1}\,\Delta\rho\,\Delta z) / (\Delta\mathbf{u} \bullet \Delta\mathbf{u})$

The Obukhov Length

Multiplying TKE eqn by $(-\kappa z/u_*^3)$, assume constant flux distribution in the surface layer, where κ is Von Karman constant 0.35~0.42

$\ldots\ldots\ldots(-\kappa z/u_*^3)\,[-(w'\mathbf{u}')_s \bullet \partial\mathbf{u}/\partial z - g(\rho' w')_s/\rho - \partial(w'e + w'p'/\rho)/\partial z - \varepsilon]$

$\xi = z/L = (-\kappa z g \rho' w')/(\rho u_*^3)$, $L = -(\rho u_*^3) / [\kappa g (\rho' w')_s]$

L can be interpreted as that proportional to the height above the surface at which buoyancy first dominate over mechanical (shear) production of turbulence.

$\xi = z/L = (-\kappa z\, w_*^3)/(z u_*^3)$ is a stability parameter

Exam 1. October 2, 2002

From the momentum equation

$\partial u_i/\partial t + u_j\partial u_i/\partial x_j + 2\varepsilon_{ijk}\Omega_j u_k = -\rho^{-1}\partial p/\partial x_i - \partial\Phi/\partial x_i + \rho^{-1}\partial\tau_{ij}/\partial x_j$

where components of the angular velocity of the earth's rotation vector Ω_j are (0, ωcosφ, ωsinφ) where φ is latitude and $\omega = 2\pi / 24\text{ hr} = 7.27 \times 10^{-5}\ s^{-1}$

Coriolis parameter $f=2\omega\sin\varphi$, $f_c=2\omega\cos\varphi$

$\tau_{ij} = \mu(\partial u_i/\partial x_j+\partial u_j/\partial x_i)+(\mu-\mu_B)\partial u_k/\partial x_k\,\delta_{ij}$

μ: dynamic viscosity, $\nu = \mu/\rho$ kinematic viscosity, μ_B ~bulk viscosity coefficient

Adopting the convention, **V** = (**u**, w) = ($u=u_1$, $v=u_2$, $w=u_3$)

1. Express the equation $\partial u_i/\partial x_i=0$ in terms of u, v, w and also in vector form
2. Assuming $\mu_B \sim 0$ & incompressibility ($\partial u_i/\partial x_i=0$)

   explain why $\rho^{-1}\partial\tau_{ij}/\partial x_j \approx \nu\partial^2 u_i/\partial x_j^2$
3. Please write the momentum equation in terms of u, v, w separately.
4. Express the horizontal momentum equation in vector form
5. From the horizontal momentum equation, derive the following equation

$d\mathbf{u}/dt + f\,\mathbf{k}\times\mathbf{u} - \rho^{-1}\partial t/\partial z = -\rho^{-1}\nabla p$, where **u** is horizontal $\quad t \approx -\rho(\mathbf{u}'w' - \nu\partial\mathbf{u}/\partial z)$

6. From the following non-dimensional form, e

$[\partial/\partial t^* + \mathbf{u}^*\cdot\nabla^* + w^*\partial/\partial z^* - (\partial^2/\partial z^{*2})]\,\mathbf{u}^* + \partial(\mathbf{u}'w')/\partial z \quad = \quad f\,\mathbf{k}\times(\mathbf{u}^* - \mathbf{u}_g^*)$

[ω/f U/fL ν/D²f]

explain the physical meaning of the following numbers

Reynolds number: $Re = UL/\nu$

Rossby number: $Ro = U/fL$

Ekman number: $Ek = \nu/D^2 f = Ro/Re\,(D/L)^2$

Home work 1 October 2, 2002

Due: Oct. 17, 2002

1. An array of thermisters measured the temperature field at 200 m as sketched below.

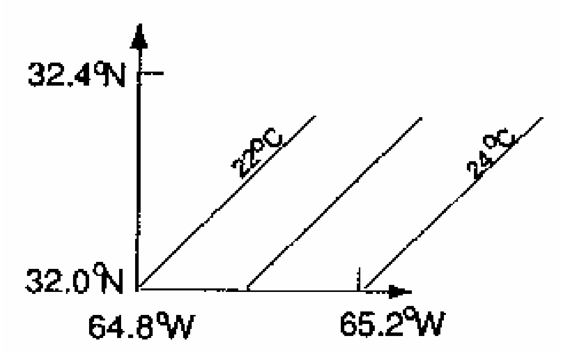

a) What is $\partial T/\partial x$, $\partial T/\partial y$?

b) What are the magnitude and direction of the horizontal vector, $\nabla T = \mathbf{i}\, \partial T/\partial x + \mathbf{j}\, \partial T/\partial y$?

c) Assume that $DT/Dt = 0$ and $w = 0$. What is $\partial T/\partial t$ if a current meter measures a constant velocity of (10 km/day, 10km/day)?

d) Why is this a good place to make measurements?

2. If $u(x, t) = a\,x$ is the steady, *Eulerian* velocity field, find Du/Dt and $x_p(X, t)$, the acceleration and position of a particle initially located at $x_p = X$ when $t = 0$.

3. Calculate the deflection due to the *Coriolis* acceleration of a baseball traveling a distance of 60 ft. at a speed of 50 mph. Let $f = 10^{-4}$ s^{-1}. (Assume that the velocity perturbations due to the *Coriolis* accelerations are small.

4. On a planet (not in our solar system) rotating at a speed $\Omega = 10^{-2}$ s^{-1}, typical atmospheric (relative) velocities are 100 m s^{-1}. Roughly, how big should the planet be before relative acceleration can be neglected in favor of *Coriolis* acceleration.

5. For steady flow, the compressible form of the continuity equation is

$$\partial(\rho u)/\partial x + \partial(\rho v)/\partial y + \partial(\rho w)/\partial z = 0$$

which can also be written

$$\partial u/\partial x + \partial v/\partial y + \partial w/\partial z + \rho^{-1}(u\partial\rho/\partial x + v\partial\rho/\partial y + w\partial\rho\,/\partial z) = 0$$

Do a scale analysis [$u = O(u_0)$, $\partial(\quad)/\,\partial x = O(L^{-1})$, etc.] on this equation to show that, if $\delta\rho/\rho \ll 1$ where $\delta\rho$ is the order of magnitude of changes in ρ, then the last three terms in the above equation can be neglected.

6. If $\mathbf{A} = 6\,\mathbf{i} + 2\,\mathbf{j}$ and $B = 2\,\mathbf{i} - 2\,\mathbf{j}$, what is **A. B?** Determine a new x–component of **B** so that the two vectors are orthogonal.

7. To derive *Gauss'* theorem, first note that the following control volume integral may be equated to a surface integral upon integration with respect to x.

$$\iiint (\partial u/\partial x)\, dxdydz = \iint (u_+ - u_-)\, dydz$$

The subscripts, + and – denote values on the two bounding surfaces of the control volume pierced by the x-coordinate at a common value of (x, z). Next, note that $u_+ = \mathbf{V}.\ \mathbf{i}$ and $u_- = -\mathbf{V}.\ \mathbf{i}$ so that

$$\iiint (\partial u/\partial x)\, dxdydz = \iint \mathbf{V}.\ \mathbf{i}\, dydz$$

where the circle in the center of the double integral sign denotes the fact that we include the entire surface surrounding the control volume. By adding similarly derived identities, we have

$$\iiint \{(\partial u/\partial x) + (\partial v/\partial y) + (\partial w/\partial z)\}\, dxdydz = \iint \mathbf{V}.\ (\mathbf{i}\, dydz + \mathbf{j}\, dxdz + \mathbf{k}\, dxdy)$$

To simplify nomenclature, let the volume element, $dx\, dy\, dz = dV$, and a surface area element, $\mathbf{i}\, dydz + \mathbf{j}\, dxdz + \mathbf{k}\, dxdy = \mathbf{n}\, dA$ where $\mathbf{n} = \mathbf{i}\, n_x + \mathbf{j}\, n_y + \mathbf{k}\, n_z$ is the unit vector normal to the area element. Then the above equation may be written in the familiar form.

$$\iiint \nabla.\ \mathbf{V} dV = \iint \mathbf{V}.\ \mathbf{n} dA$$

Make a sketch of all the steps in this derivation. Interpret n_x, n_y, n_z and show that $n_x + n_y + n_z = 1$.

8. The equation in the preceeding problem may be easily generalized so that

$$\iiint \nabla.\ (P\mathbf{V}) dV = \iint P\mathbf{V}.\ \mathbf{n} dA$$

where P is any scalar quantity. Using this equation and a combination of equations (2-2) and (2-20), show that

$$\partial/\partial t \iiint S dV + \iint S\mathbf{V}.\ \mathbf{n} dA = -\iint \mathbf{j}.\ \mathbf{n} dA$$